ACADEMIA ROMÂNĂ
Revue Roumaine de Chimie
http://web.icf.ro/rrch/

Rev. Roum. Chim.,
2021, *66*(12), 921–930
DOI: 10.33224/rrch.2021.66.12.05

PERFORMANCE OF ETHANOLIC EXTRACT PROPOLIS AS A SAFE INHIBITOR FOR AA7075 ALLOY CORROSION IN NEUTRAL CHLORIDE MEDIUM

Meryem ACILA,[a] Hakim BENSABRA[b*] and Adel SAOUDI[c,d]

[a] Materials Environment Interactions Laboratory (LIME), University of Mohamed Seddik Benyahia, Ouled Aïssa, BP 98, Jijel 18000, Algeria
[b] Laboratory of Applied Energetics and Materials (LEAM), University of Mohamed Seddik Benyahia, Ouled Aïssa, BP 98, Jijel 18000, Algeria
[c] CRAPC Center for Scientific and Technical Research in Physico-Chemical Analysis, Bou-Ismail Industrial Zone, Tipaza, PO 384, RP 42001, Algeria
[d] Metallurgy and Materials Engineering Laboratory (LMGM), BADJI Mokhtar - Annaba University PO 12, CP 23000, Algeria

Received November 20, 2021

Ethanolic extract of Algerian propolis (EEP) was tested as an eco-friendly corrosion inhibitor for AA7075 alloy in 3% NaCl solution using gravimetric studies, electrochemical measurements and surface analysis. The results indicate that the addition of EEP decreases significantly the corrosion rate of AA7075 alloy, with efficiency proportional to the inhibitor concentration. The maximum percentage inhibition efficiency of 83,31% was obtained at concentration of 500 ppm. Potentiodynamic polarization analysis considered EEP as mixed type inhibitor. Electrochemical impedance spectroscopy tests revealed the presence of a protective layer on the metal surface. Scanning electron microscopy analysis confirms the existence of protective film on the alloy's surface due to the adsorption of the inhibitor molecules obeying Langmuir adsorption isotherm.

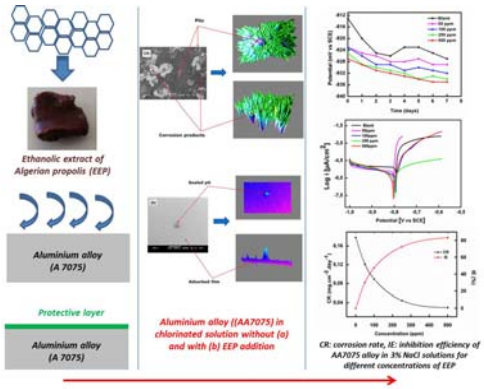

INTRODUCTION

Corrosion is a degradation phenomenon of materials (metallic in general) by the environment.[1] It is therefore a phenomenon which concerns most industrial sectors, notably the aeronautical industry, the nuclear sector, the automobile industry and the chemical and petrochemical industries.[2]

Aluminum and its alloys represent an important category of materials. Thermodynamic data show that aluminum is an eminently oxidizable metal.[3] This statement seems to be contradicted by daily experience, which attests that this metal is unalterable in the air, even at high temperatures. This enigma is explained by the formation of a thin oxide layer of alumina, very adherent and very compact.[4]

The use of inhibitors is a very practical method to protect metals against corrosion in aggressive environment. Corrosion inhibitors are molecules which reduce or stop the dissolution of metal, when added at low concentrations in corrosive media.[5-7]

Most synthetic compounds have good anti-corrosion action, but their synthesis is often very expensive. These inhibitors are toxic and can cause

* Corresponding author: h.bensabra@univ-jijel.dz; Tel.: +213792295013; Fax: +21334501189

serious damages to humans and the environment.[8-9] Therefore, natural compounds are classified as most promising eco-friendly corrosion inhibitors.[10-12] They are used for the protection of metals instead of toxic compounds. Moreover, the extraction procedure from plants is very simple and at low cost.[13] In addition to plant extracts, beekeeping products are another type of natural compounds that have been used effectively to protect metals from corrosion. Previous works have already demonstrated the excellent anticorrosive efficacy of honey on several metals such as: copper,[14] zinc,15 c-steel[16] and CuNiFe alloys.[17]

Propolis is a resinous matrix synthesized by bees from bark, buds, conifers and other trees. Bees use propolis to build their hives. This very sticky material contains a lot of active molecules especially phenolic compounds which have therapeutic properties. [18]. Recent studies on propolis have shown the effectiveness of EEP against cancer therapy.[19.20]

For the first time, the present work aims to investigate the effect of ethanolic extract of Algerian propolis (EEP) as potent green corrosion inhibitor on the corrosion behaviour of AA7075 alloy in neutral chloride solution using gravimetric and electrochemical methods including open circuit potential, potentiodynamic polarization and impedance spectroscopy. The morphology of the metal surface after immersion in the aggressive environment without and with inhibitor addition was analysed by scanning electron microscopy (SEM).

MATERIALS AND METHODS

1. Electrodes Preparation

AA7075 aluminum alloy had the following chemical composition (wt.%): Cu 1.51, Mg 2.62, Mn 0.24, Ti 0.015, Zn 5.99, Fe 0.42, Si 0.068 and the remainder aluminum. Disc electrodes were cut from a cylindrical rod 11 mm in diameter. The electrodes were connected to a copper wire and mounted in an epoxy resin with an exposed area of 0.87 cm^2. Prior to each electrochemical experiment, the electrodes surfaces were abraded using emery papers (between 180 and 2000 grades), washed with acetone, rinsed with distilled water, and dried in air.

2. Electrolyte Composition

The corrosion behaviour of AA7075 alloy was studied in neutral chloride solution (3% NaCl) with and without inhibitor addition. Propolis collected from Jijel (Algeria), was used in this study. The preparation of ethanolic extract and the identification of its composition have been described by Lahouel *et al.*[21] The chemical composition of propolis can change depending on the plants the bees visit. However, even if the compositions differ, propolis still retains the same virtues. In general, propolis has the following composition: tree resin (flavonoids, esters, phenolic acids, etc.), wax, essential oils, pollen and various substances. The main compounds in the ethanolic extract are flavonoids.[22,23] The major flavonoids detected were: pinostrobin, chalcone, pinocembrin, chrysin and naringenin.

The used concentrations of the inhibitor were 50, 100, 250 and 500 ppm.

3. Gravimetric study

Gravimetric measurements were performed using aluminum alloy samples immersed in the beakers containing the electrolyte without and with different concentrations of the inhibitor (50-500). The samples of aluminum alloy (size 1.1 cm × 0.2 cm) were abraded with silicon carbide paper (600, 800 and 1200 grids), rinsed with deionized water and then degreased in acetone. The samples were then immersed in aerated solutions for 3 days. The temperature of the testing solutions was maintained at 25 °C. The cleaned samples were weighed before and after immersion to determine the weight loss. The corrosion rate was calculated using the equation (1):[24]

$$CR = \frac{m_1 - m_2}{S \cdot t} \quad (1)$$

where: m_1 and m_2 are the masses of the samples before and after immersion respectively in (g), S is the area of the specimen in (cm^2) and t is the exposure time in days.

The surface coverage (θ) and the percentage inhibition efficiency (IE) were calculated using the equations (2) and (3), respectively:[25-27]

$$\theta = \frac{CR_0 - CR}{CR_0} \quad (2)$$

where CR_0 and CR are the corrosion rates of the samples without and with inhibitor addition, respectively.

$$IE = \frac{CR_0 - CR}{CR_0} \cdot 100 \quad (3)$$

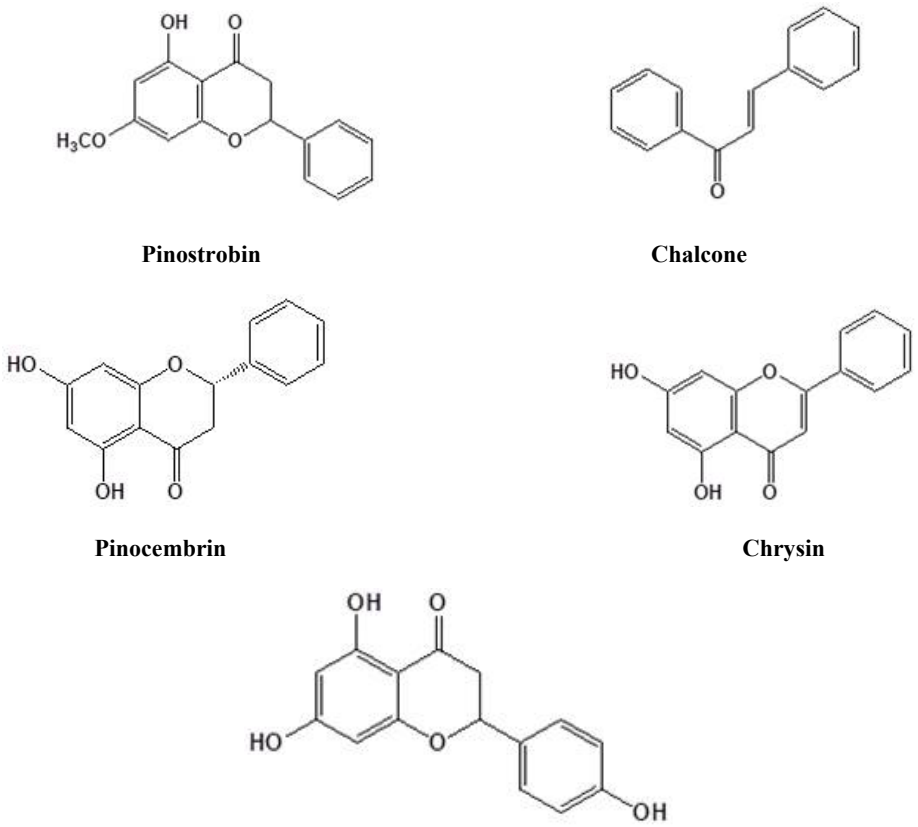

Fig. 1 – Chemical formulas of the most abundant flavonoids from EEP.

4. Electrochemical tests

The electrochemical experiments were acquired using a Radiometer Analytical Voltalab 40 PGZ301 potentiostat/galvanostat controlled by Voltamaster 4 software. The electrodes were tested using a standard three electrode cell with AA7075 alloy as the working electrode, platinium mesh as counter and saturated Calomel electrode (SCE) as reference.

Potentiodynamic curves were obtained after 1 h of immersion in the test electrolyte, without and with inhibitor addition, under scan rate of 0.25 mV s^{-1}. Electrochemical impedance spectroscopy (EIS) measurements were performed at frequencies ranging from 100 kHz to 10 mHz using an applied AC signal of 10 mV at the OCP. The data were analysed and fitted using ZSimpWin software.

5. Surface Analysis

The surface states of the samples immersed in 3% NaCl solutions with and without inhibitor, were observed by scanning electron microscope (SEM) model Jeol 6360LV. Before immersion, the samples were polished with silicon carbide paper of different grade numbers (120 to 1200). They were further polished with diamond paste to obtain a near mirror surface. After 7 days of immersion, coupons were retrieved, rinsed with distilled water, dried and analyzed immediately.

RESULTS AND DISCUSSION

1. Weight loss test

The percentage inhibition efficiency and the corrosion rate for different concentrations of EEP calculated from weight loss are shown in Figure 2. As can be seen from Table 1, at all concentrations, EEP inhibits corrosion of the samples. Corrosion rates decreased with an increase in inhibitor concentration. As the concentrations of the inhibitor increase, the surface coverage values increase and acquire the highest value of (0.8331).The values of the percentage inhibition efficiency (IE) indicate that EEP exhibits a significant inhibitory effect on the corrosion of AA7075 alloy in 3% NaCl solution. The addition of 500 ppm of EEP enhances the inhibition efficiency to 83.31%.

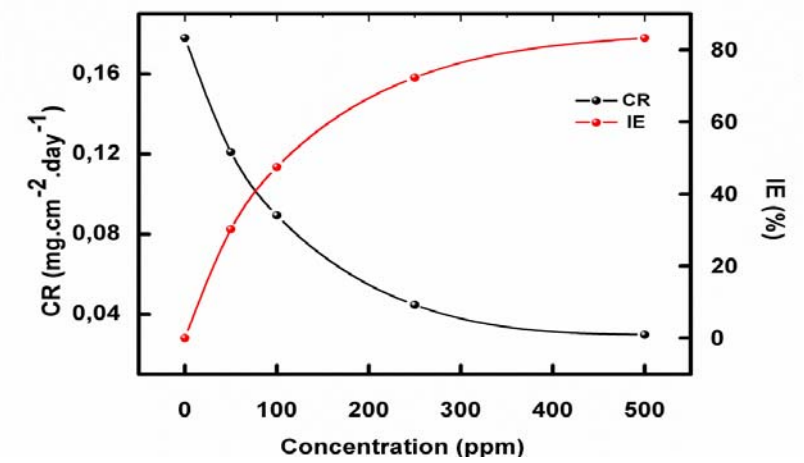

Fig. 2 – Evolution of the corrosion rate (CR) and inhibition efficiency (IE) of AA7075 alloy in 3% NaCl solutions for different concentrations of EEP.

Table 1

Corrosion rate and inhibition efficiency for AA7075 alloy in chlorinated solutions with different concentrations of EEP obtained from gravimetric measurements

	C_{inh} (ppm)	CR ($mg.cm^{-2}.day^{-1}$)	θ	IE (%)
Blank	0	0.1780	0	0
EEP	50	0.1210	0.3020	30.20
	100	0.0893	0.4746	47.46
	250	0.0446	0.7232	72.32
	500	0.0297	0.8331	83.31

2. Open circuit potential measurement

Figure 3 represents the effect of EEP on the corrosion potential evolution of AA7075 alloy immersed 3% NaCl solution for 7 days.

It can be observed that, the blank exhibits the highest values of corrosion potential (-825 mV/SCE). In the presence of EEP at different concentrations, the corrosion potential becomes more negative with time (in the range of -828 to -834 mV/ SCE). This effect is more evident at prolonged immersion times and with higher inhibitor concentration. The slight shift in the potential for the samples with and without inhibitor addition suggests that EEP is a mixed-type inhibitor. Therefore, it acts on the anodic and cathodic sites to inhibit the electrochemical reactions.[28-30]

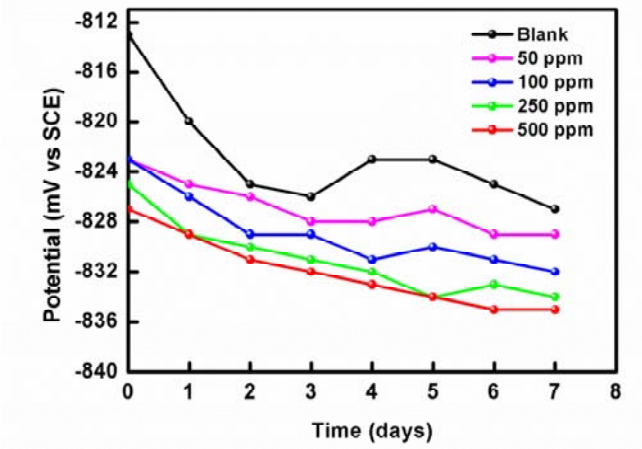

Fig. 3 – Corrosion potential evolution of aluminum alloy immersed in the 3% NaCl solution with and without EEP addition.

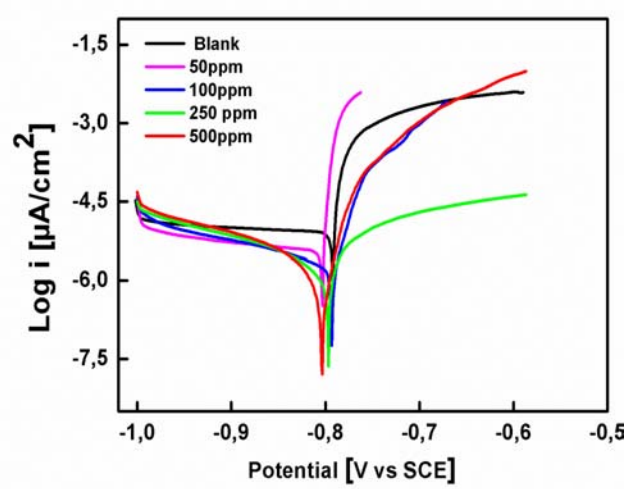

Fig. 4 – Potentiodynamic polarization curves for AA7075 alloy immersed for 60 min in 3% NaCl solutions without and with different concentrations of EEP.

3. Polarization curves

Figure 4 depicts potentiodynamic Polarization curves of AA7075 alloy in the electrolyte without and with the various concentrations of EEP.

The analysis of polarization curves indicates that the addition of EEP decreases the corrosion current density (i_{corr}) and the corrosion rate. Electrochemical parameters deduced from the polarization curves are shown in Table 2. The addition of EEP did not make significant changes in the corrosion potential values with respect to the blank. This allows us, according to the literature, to classify it as a mixed type inhibitor. Both anodic and cathodic polarizations are influenced simultaneously.[31-34] The corrosion current density (i_{corr}) decreases with increasing the concentration of EEP. When the adding amount of inhibitor was 500 ppm; i_{corr} was the lowest with the value of $8.7.10^{-2}$ µA/cm^2 and inhibition efficiency reached 89.26%. The percentage inhibition efficiency was estimated using equation (4):

$$IE = \frac{i^{\circ}_{corr} - i_{corr}}{i^{\circ}_{corr}} x100\% \quad (4)$$

where i°_{corr} and i_{corr} are the corrosion current densities without and with inhibitor addition, respectively.

The percentage inhibition efficiency IE (%) increased with the increase in the concentration of EEP. These results indicate the adsorption of active molecules and the formation of a protective film on the alloy surface by blocking the corrosion reaction centers.[31-35]

The major flavonoids detected in the ethanolic extract were: pinostrobin, chalcone, pinocembrin, chrysin and naringenin. For the anodic branch, the inhibition may be due to the adsorption of flavonoids through oxygen atoms or ring oxygen atom and forms a protective layer on the metal surface, thus prevents the contact between the metal and the electrolyte.

The protonated species of the principle constituents may compete with H^+ ion reduction and may control the cathodic reaction.

Table 2

Tafel polarization parameters of AA7075 alloy in 3% NaCl solution at different concentrations of EEP

Concentration (ppm)	E_{corr} (mV vs SCE)	i_{corr} (µA/cm²)	R_p (Ω.cm²)	IE (%)
0	-793	$8{,}1 \cdot 10^{-1}$	836.28	-
50	-802	$5.7 \cdot 10^{-1}$	3430	29.63
100	-791	$2{,}3 \cdot 10^{-1}$	3760	71.60
250	-792	$1.3 .10^{-1}$	5480	83.95
500	-805	$8.7 \cdot 10^{-2}$	11750	89.26

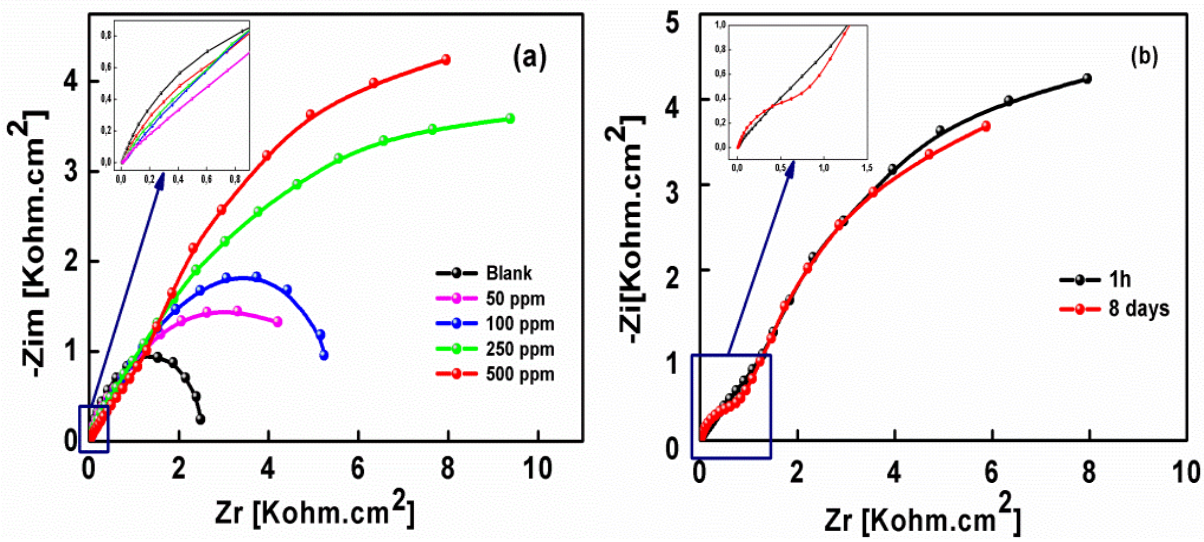

Fig. 5 – Impedance spectra reflecting the effect of EEP on the behavior of AA7075 alloy in 3% NaCl solution: (a) after 1 hour of immersion, (b) effect of the immersion time for a concentration of 500 ppm.

4. Electrochemical impedance spectroscopy (EIS)

Figure 5 shows the EIS results after 1 h and 8 days immersion of aluminum alloy in neutral chloride solutions with different concentrations of EEP.

The impedance spectra of the sample without inhibitor represent a depressed semicircle. In the presence of EEP at different concentrations, the spectra exhibit two semicircles capacitive loops with two different time constants. The first one is higher frequency loop (HF) which is usually attributed to the aluminum oxide film and/or inhibitor deposit. The second one at low frequency is generally assigned to the charge transfer process.[35,36] From the recorded diagrams, it is clearly seen that the EIS measurements confirm the inhibitory efficiency of EEP already proven by potentiodynamic polarization. Figure 5 (a) shows that the presence of EEP improved the corrosion resistance of AA7075 alloy. The diameter of the semicircles increase with the increase in the inhibitor concentration. Figure 6 shows the equivalent circuits used to fit the experimental data. These circuits, with two time constants, can provide insight to understand the phenomena taking place at the electrochemical interface. The corresponding best fitting parameters are reported in Table 3. This model was used by many authors to describe the behavior of aluminum alloys in 3% NaCl solutions [37-42]. The used circuits are formed by the following elements: R_e is the resistance of the electrolyte, R_1 the resistance of the film, *CPE1* is the constant phase element describing the film capacitance, CPE2 is the constant phase element which describes the double layer capacitance and R_2 is the charge transfer resistance.

The CPE1 and CPE2, are used in place of the ideal capacitive elements in order to consider the inhomogeneous nature of the electrode surface.[43]

Thus, we see that the semicircle loop of the sample immersed in chloride solution without inhibitor addition present a lowest diameter which correspond to the lowest value of the film resistance (around 5,9E3 Ω.cm²) coupled to the highest value of the film capacitance Q_f (around 49.5E-6 S.s^n/cm²), as listed in Table 3. This can be explained by the local destruction of the oxide film (Al_2O_3) followed by a continuous dissolution of the aluminum in contact with the aggressive solution (pitting attack).

In inhibitor-containing solution, the diameter of the obtained capacitive loops increases with increasing concentration. This corresponds to a decrease in corrosion rate. This fact can be explained by the growing adsorption of the inhibitor molecules on the alloy surface (anodic and cathodic sites) which induces the inhibition of partial electrochemical reactions. This inhibitive effect is quite reflected by the values of the fitting data listed in Table 3. Therefore, in the presence of EEP, the double layer capacitance (Q_{dl}) decreases to 4.91.E-5 S.s^n/cm² and the resistance (R_{ct}) passes to 6.400.E3 Ωcm². The film resistance for the blank has value equal to 5.900.E3 Ωcm². However, it is increased to 1.310.E4 Ω.cm² with the addition of EEP for a concentration equal to 500 ppm. Coupled to this increase in R_f, the film capacitance (Q_f) decrease with the presence of the inhibitor, it passes from a value of 49.5.E-6 S.s^n/cm², for the blank, to a value of 1.116.E-5 S.s^n/cm². A decrease in the value of capacitance can be explained by the formation of a protective layer on the alloy surface.[44]

Table 3

EIS parameters for AA7075 alloy in 3%NaCl solution with different concentrations of EEP

Concentration (ppm)	R_e ($\Omega.cm^2$	CPE1 ($S.s^n/cm^2$)	R_1 ($\Omega.cm^2$)	n_1	R_2 ($\Omega.cm^2$)	CPE2 ($S.s^n/cm^2$)	n_2	X^2
0 (1h)	16.75	$49.5 \cdot 10^{-6}$	5900	0.803	262	$64.79 \cdot 10^{-6}$	0.96	79.10^{-4}
50	18.69	$5.17 \cdot 10^{-6}$	6750	0.877	2730	$3.975 \cdot 10^{-6}$	0.85	48.10^{-4}
100	19.55	$2.135 \cdot 10^{-6}$	7200	0.85	3800	$1.674 \cdot 10^{-6}$	0.86	35.10^{-4}
250	19.36	$3.151 \cdot 10^{-5}$	10300	0.86	5200	$4.697 \cdot 10^{-5}$	0.86	45.10^{-4}
500	19.61	$1.116 \cdot 10^{-5}$	13100	0.86	6400	$4.091 \cdot 10^{-5}$	0.87	41.10^{-4}
500 (8 days)	18.55	$1.874 \cdot 10^{-6}$	13200	0.84	6460	$2.566 \cdot 10^{-6}$	0.84	37.10^{-4}

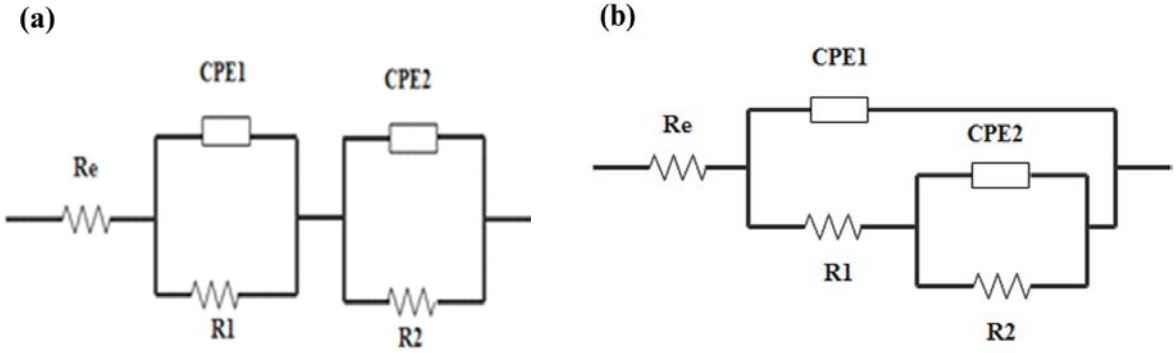

Fig. 6 – Equivalent Electrical Circuits used to fit the impedance data for Al7075 alloy in chloride media without (a) and with (b) EEP addition.

The impedance of CPE is determined by the equation below:

$$Z_{CPE} = (Q(J\omega)^n)^{-1} \quad (5)$$

where Q is the CPE with dimensions of $S.s^n.cm^{-2}$; ω is the angle frequency in $rad.s^{-1}$; and n is the CPE exponent. Generally, n ranges between 1 (pure capacitor) and 0.5 (ideal resistor).[45,46] After taking account the inhomogeneity of the electrode surface, the real capacitance is determined by the formula:

$$C = Q(\omega_{max})^{n-1} \quad (6)$$

where ω_{max} is the maximum frequency, at which the imaginary component of the Nyquist plot is maximum.

The Nyquist plots of the AA7075 alloy obtained after 1 hour and 8 days of immersion in 3% NaCl solutions containing 500 ppm of EEP are displayed in FIG. (5b). The superposition of the two semicircles indicates that the passive film formed remains stable with time.

5. Adsorption isotherms

The surface coverage (θ) values, obtained from weight loss measurements, were used to study the adsorption mechanism of EEP.

According to Langmuir's isotherm, θ is related to the inhibitor concentration by the equation (5):

$$\frac{C_{inh}}{\theta} = \frac{1}{K_{ads}} + C_{inh} \quad (7)$$

where C_{inh} is the inhibitor concentration and K_{ads} is the adsorptive equilibrium constant.

The plot of C_{inh}/θ vs C_{inh} is linear (Figure 3) and the correlation coefficient (R^2) is close to 1. This indicates that the adsorption of the product obeys Langmuir isotherm model. The value of the equilibrium constant (K_{ads}) has been calculated. It is related to the standard free energy of adsorption $\Delta G°_{ads}$ by the relation below:

$$K_{ads} = \frac{1}{55,5} e^{\frac{-\Delta G_{ads}}{R.T}} \quad (8)$$

The value 55.5 is the molar concentration of water, R is the universal gas constant in J. mol^{-1}. K^{-1} and T is the temperature in K.

As it is mentioned in the literature, Langmuir isotherm is based on the assumption that all the adsorption sites are equivalent and the molecules binding occurs independently from nearby sites being occupied or not, this might not be true in the case of propolis extract since it contains various organic molecules having polar atoms or functional groups from heterocyclic compounds which might interact one another. Consequently, we have to note that the value of ΔG_{ads} is not enough to discuss and understand the adsorption isotherm mechanism of EEP, because the composition of the extract is not known and therefore the molecular mass is unknown.[25,31,47]

6. Surface analysis

Figure 8 shows the SEM images of aluminum surface obtained after 7 days exposure in 3% NaCl solution with and without EEP addition. The obtained images were analyzed using the image processing software "ImageJ 1.53K" in order to highlight the depth of the corrosion pits as well as the morphology of the formed corrosion products and of the deposited films on the metallic surface.

As can be seen, the SEM images confirm the results obtained electrochemical analysis concerning the effect of chlorides and inhibitor addition on the surface condition of aluminum alloy. Thus, we note that the surface of samples immersed in chlorinated solution free of inhibitors, Figure 8(a), had a severe attack reflected by the formation of a large number of corrosion pits as well as the formation of a large amount of corrosion product (aluminum hydroxide) resulting from the dissolution of the metal matrix. Nevertheless, in the presence of the ethanolic extract of propolis at a concentration of 500 ppm, Figure 8(b) show that the aluminum alloy matrix is more or less unattacked, without any severe corrosion attack by the medium. We can observe the presence of adsorbed film on the metallic surface and the total absence of pits induced by chlorides attack. The adsorption of the inhibitor on the alloy surface generates consistent protective layers, which acts as a physical barrier between the metallic surface and the aggressive ions dissolved in the solution.

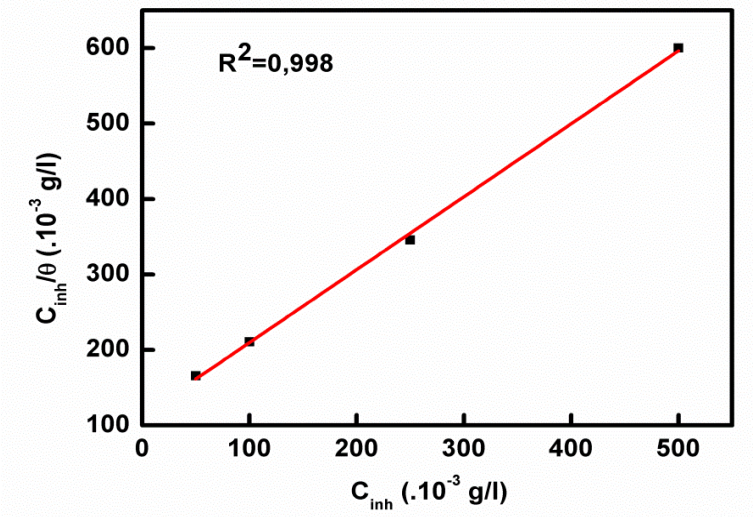

Fig. 7 – Langmiur adsorption isotherm of EEP in 3% NaCl for AA7075 alloy at 298°K.

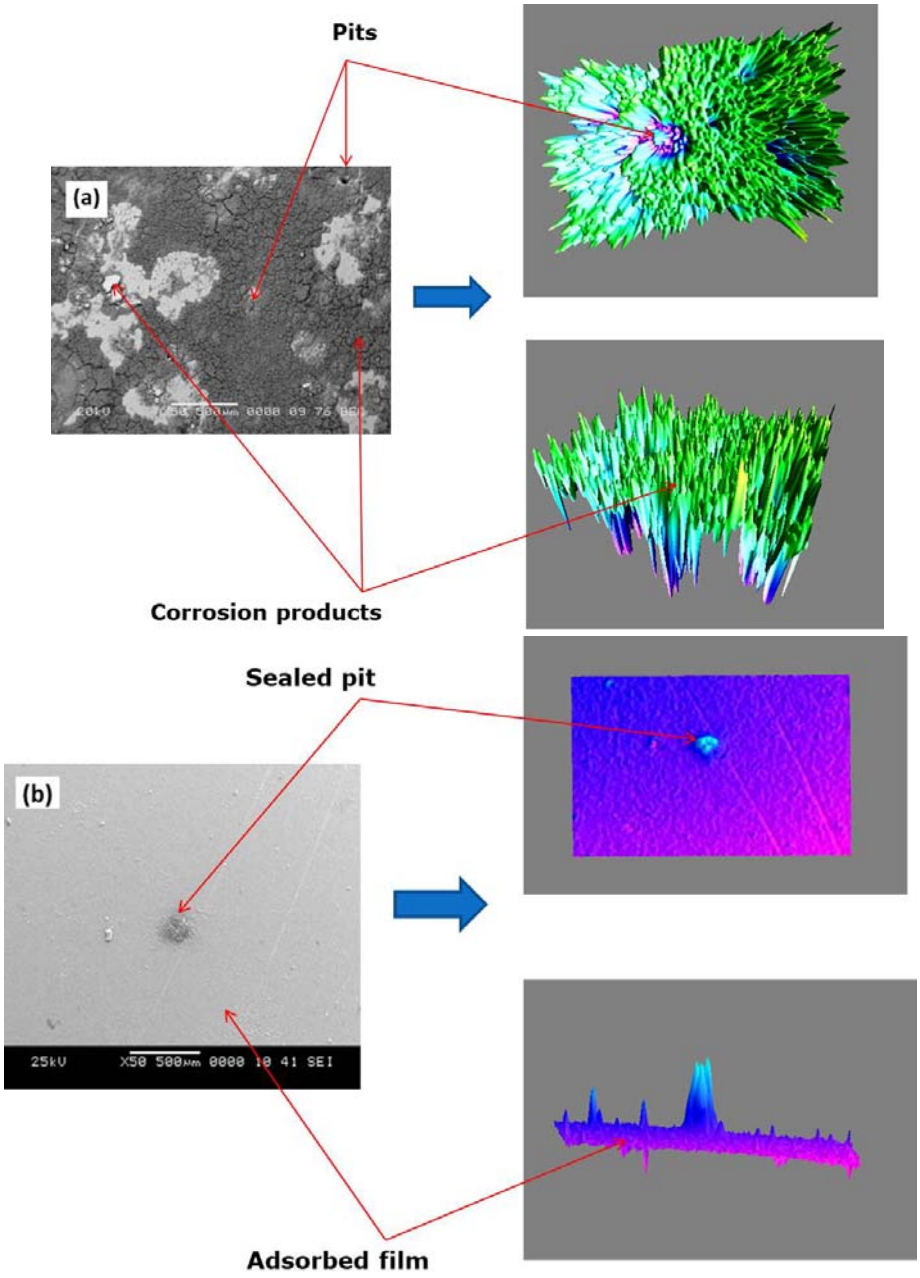

Fig. 8 – SEM images of AA7075 alloy after 7 days immersion in 3% NaCl solutions without (a) and with the presence of 500 ppm of EEP (b).

CONCLUSION

Ethanolic extract of propolis (EEP) was tested as an efficient corrosion inhibitor for AA7075 alloy in neutral chloride solution using gravimetric and electrochemical methods (Open circuit potential, polarization curves and electrochemical impedance spectroscopy). Surface morphology was analyzed by scanning electron microscopy (SEM). From the obtained results, we can conclude that:

Gravimetric studies show that the addition of EEP slows the corrosion process of the aluminum alloy and increases the percentage inhibition efficiency with the increase in inhibitor concentration to reaches a maximum value of 83.81%.

Polarization curves show that ethanolic extract of Algerian propolis (EEP) may be classified as mixed type inhibitor.

The obtained EIS spectra proved that ethanolic extract of Algerian propolis inhibit successfully the corrosion of AA7075 alloy by the formation of a protective layer stable during time.

The inhibitor was adsorbed on the aluminum alloy surface and follows the Langmuir isotherm model. SEM images confirm the ability of ethanolic extract of Algerian propolis to retard the

corrosion of AA7075 alloy by the formation of an adherent and compact film on the metal surface.

Acknowledgments. The authors are grateful to Pr Mesbah LAHOUEL from Laboratory of Molecular Toxicology, university of Jijel, for the consistent support.

REFERENCES

1. Z. Tang, *Curr. Opin. Solid State Mater. Sci.***, 2019**, *23*, 100759.
2. H. Keles, M. Keles, I. Dehri and O. Serindag, *Colloids. Surf. A. Physicochem. Eng. Asp*., **2008**, *320*, 138-145.
3. R. Rosliza, W. B. Wan Nik, S. Izman and Y. Prawoto, *Curr. Appl. Phys.,* **2010**, *10*, 923-929.
4. D. Prabhu and P. Rao, *J. Environ. Chem. Eng.*, **2013**, *1*, 676-683.
5. M. Lebrini, F. Robert and C. Roos, *Int. J. Electrochem. Sci.*, **2011**, *6*, 847 – 859.
6. G. Ji, S. Anjum, S. Sundaram and R. Prakash, *Corros. Sci*., **2015**, *90*, 107-117.
7. M. Yishnudevan and K. Thangavcl, *Indian J. Chem. Technol.*, **2007**, *14*, 22-28.
8. I. Radojcic, K. Berkovic, S. Kovac and J. Vorkapic-Furac, *Corros. Sci.*, **2008**, *50*, 1498-1504.
9. S. Marzorati, L. Verotta and S. P. Trasatti, Molecules, **2019,** *24*, 48-54.
10. I. M. Chung, R. Malathy, S. H. Kim, K. Kalaiselvi, M. Prabakaran and M. Gopiraman, *J. Adhes. Sci. Technol.*, **2020**, *34*, 1483-1506.
11. J. Halambek, A. N. Grassino and I. Cindrić, *Int. J. Electrochem. Sci.*, **2020**, *15*, 857- 867.
12. N. Raghavendra, *J. Bio. Tribo. Corros.*, **2019,** *5*, 1-19.
13. A. Sedik, D. Lerari, A. Salci, S. Athmani, K. Bachari, İ. Gecibesler and R. Solmaz, *J. Taiwan. Inst. Chem. Eng*., **2020**, *107*, 189-200.
14. A. Y. El-Etre, *Corros. Sci.*, **1998**, *40*, 1845-1850.
15. A. O. Odiongenyi, I. S. Enengedi, I. Ibok and E. J. Ukpong, *Int. J. Chem. Mater. Environ. Res.*, **2015**, *2*, 16-25.
16. A. Y. El-Etre and M. Abdallah, *Corros. Sci.*, **2000**, *42,* 731-738.
17. L. Vrsalovic, S. Gudic and M. Kliskic, Ind. J. Chem. Technol., **2012**, *19*, 96-102.
18. J. Ryl, J. Wysocka, M. Cieslik, H. Gerengi, T. Ossowski, S. Krakowiak and P. Niedzialkowski, *Electrochim Acta*, **2019**, *304*, 263-274.
19. L. Benguedouar, M. Lahouel, S. C. Gangloff, A. Durlach, F. Grange, P. Bernard, F. Antonicelli, *Anticancer Agents Med. Chem.*, **2016**, *16*, 1172-1183.
20. H. Brihoum, M. Maiza, H. Sahali, M. Boulmeltout, G. Barratt, L. Benguedouar and M. Lahouel, *Braz. J. Pharm. Sci.*, **2018**, *54*, e17396.
21. K. Boutabet, W. Kebsa, M. Alyane and M. Lahouel, *Indian. J. Nephrol.*, **2011,** *21*. 101-106.
22. N. Zabaiou, A. Fouachea, A. Trousson, S. Baron, A. Zellagui, M. Lahouel and J. M. A. Lobaccaro, *Chem. Phys. Lipids*, **2017,** *207*, 214-222.
23. L. Benguedouar, H. N. Boussenane, W. Kebsa, M. Alyane, H. Rouibah and M. Lahouel, *Indian. J. Exp. Biol.*, **2008**, *46*, 112-119.
24. K. F. Khaled, *Mater. Chem. Phys.,* **2008**, *112*, 104-111.
25. J. Halambek, K. Berkovic and J. Vorkapic-Furac, *Mater. Chem. Phys.*, **2013**, *137,* 788-795.
26. K. F. Khaled, *Mater. Chem. Phys*., **2011**, *125*, 427-433.
27. A. Khadraoui, A. Khelifa, K. Hachama and R. Mehdaoui, *J. Mol. Liq.*, **2016**, *214*, 293-297.
28. N. Nnaji, N. Nwaji, J. Mack and T. Nyokong, *Molecules*, **2019,** *24*, 207-214.
29. B. Zaid, N. Maddache, D. Saidi, N. Souami, N. Bacha and A. Si Ahmed, *J. Alloys. Compd.*, **2015**, *629*, 188-196.
30. B. Liu, X. Zhang, X. Zhou, T. Hashimoto and J. Wang, *Corros. Sci.*, **2017**, *126*, 265-271.
31. S. Varvara, R. Bostan, O. Bobis, L. Gaina, F. Popa, V. Mena and R. M. Souto, *Appl. Surf. Sci.*, **2017**, *426*,1100-1112.
32. K. Krishnaveni and J. Ravichandran, *J. Adhes. Sci. Technol.*, **2015**, *29*, 1465-1482.
33. U. Nazir, Z. Akhter, N. K. Janjua, M. A. Asghar, S. Kanwal, T. M. Butt, A. Sani, F. Liaqat, R. Hussain and F. U. Shah, *RSC Adv*., **2020**, *10*, 7585-7599.
34. R. S. Nathiya, S. Perumal, M. Moorthy, V. Murugesan, R. Rangappan and V. Raj, *J. Bio. Tribo. Corros.*, **2020**, *6*, 1-15.
35. Y. Qiang, S. Zhang, S. Xu and L. Yin, *RSC Adv*., **2015**, *5*, 63866-63873.
36. A. K. Mishra and R. Balasubramaniam, *Corrosion*, **2007**, *63*, 240-248.
37. K. Zhou, B. Wang, Y. Zhao and J. Liu, *Trans. Nonferrous Met. Soc. China*, **2015**, *25*, 2509-2515.
38. A. Aballe, M. Bethencourt, F. J. Botana, M. Marcos and R. Osuna, *Mater. Sci.*, **2001**, *52*, 185-192.
39. S. J. Garcia, T. A. Markley, J. M. C. Mol and A. E. Hughes, *Corros. Sci.*, **2013**, *69*, 346-358.
40. W. R. Osório, E. S. Freitas and A. Garcia, *Electrochim. Acta*, **2012**, *102*, 436- 445.
41. A. I. Stoica, J. Świątowska, A. Romaine, F. Di Franco, J. Qi, D. Mercier, A. Seyeux, S. Zanna and P. Marcus, *Surf. Coat. Technol.*, **2019**, *369*, 186-197.
42. M. Acila, H. Bensabra and M. Santamaria, *Metall. Res. Technol.*, **2021**, *118*, 203-208.
43. H. Bensabra, A. Franczak, O. Aaboubi, N. Azzouz and J. P. Chopart, *Metall. Mater. Trans. A*, **2016**, *48*, 412-424.
44. H. Bensabra and N. Azzouz, *Metall. Mater. Trans. A*, **2013**, *44A, 5*703-5710.
45. I. B. Onyeachu, I. B. Obot and A. Y. Adesina, *Corros. Sci.*, **2020**, *168*, 108589-108594.
46. H. Ma, S. Chen, B. Yin, S. Zhao and X. Liu, *Corros. Sci.*, **2003**, *45*, 867-882.
47. M. Faustin, A. Maciuk, P. Salvin, C. Roos and M. Lebrini, *Corros. Sci*., **2015**, *92*, 287-300.